Long−range transport of anthropogenic air pollutants into the marine air: Insight into fine particle transport and chloride depletion on sea salts

Liang Xu[1], Xiaohuan Liu[2], Huiwang Gao[2], Xiaohong Yao[2], Daizhou Zhang[3], Lei Bi[1], Lei Liu[1], Jian Zhang[1], Yinxiao Zhang[1], Yuanyuan Wang[1], Qi Yuan[2], Weijun Li[1,*]

[1]Department of Atmospheric Sciences, School of Earth Sciences, Zhejiang University, Hangzhou 310027, China

[2]Key Laboratory of Marine Environment and Ecology, Ministry of Education, Ocean University of China, Qingdao 266100, China

[3]Faculty of Environmental and Symbiotic Sciences, Prefectural University of Kumamoto, Kumamoto 862-8502, Japan

*Corresponding author: W. Li (liweijun@zju.edu.cn)

Abstract

Long-range transport of anthropogenic air pollutants from East Asia can affect the downwind marine air quality during spring and winter. Long-range transport of continental air pollutants and their interaction with sea salt aerosols (SSA) significantly modify the radiative forcing of marine aerosols and influence ocean biogeochemical cycling. Previous studies poorly characterize variations of aerosol particles along with air mass transport from the continental edge to the remote ocean. Here, the research ship R/V Dongfanghong 2 traveled from the eastern China seas

(ECS) to the northwestern Pacific Ocean (NWPO) to understand what and how air pollutants were transported from the highly polluted continental air to clean marine air in spring. A transmission electron microscope (TEM) was used to find the long-range transported anthropogenic particles and the possible Cl-depletion phenomenon of SSA in marine air. Anthropogenic aerosols (e.g., sulfur (S)-rich, S-soot, S-metal/fly ash, organic matter (OM)-S, and OM coating particles) were identified and dramatically declined from 87% to 8% by number from the ECS to remote NWPO. For the SSA aging, 87% of SSA particles in the ECS were identified as fully aged, while the proportion of fully aged SSA particles in the NWPO decreased to 29%. Our results highlight that anthropogenic acidic gases in the troposphere (e.g., SO_2, NO_x, and volatile organic compounds) could be transported to remote marine air and exert a significant impact on aging of SSA particles in the NWPO. The study shows that anthropogenic particles and gases from East Asia significantly perturb different aerosol chemistry from coastal to remote marine air. More attention should be given to the modification of SSA particles in remote marine areas due to the influence of anthropogenic gaseous pollutants.

1. Introduction

Marine aerosols play an important role in the global aerosol emission budget and greatly impact the Earth's radiative forcing and biogeochemical cycling (O'Dowd Colin and de Leeuw, 2007). Sea salt aerosol (SSA) is one crucial component of marine aerosols, especially in the remote marine atmosphere (Lewis and Schwartz, 2004). SSA is composed of Na and Cl with minor amounts of Mg, Ca, K, and S (Li et al., 2016a). Fresh SSA usually has the form of a cubic NaCl core associated with $MgCl_2$ and $CaSO_4$ coating (Chi et al., 2015). SSA in polluted air can serve as reactive surfaces through the uptake of acidic gaseous SO_2, NO_x, and organic acids, releasing gaseous reactive chlorine compounds (chloride depletion) (Laskin et al., 2012; Yao and Zhang, 2012). Moreover, the SSA aging processes can transform fresh SSA into partially aged SSA and finally into fully aged SSA that mainly contain $NaNO_3$, Na_2SO_4, and organic sodium salts (Chi et al., 2015; Laskin et al., 2012). These products from the chemical aging processes also modify hygroscopic properties of individual SSA (Cravigan et al., 2020; Ghorai et al., 2014). Some studies found that the aged SSA could alter global climate directly by scattering incoming solar radiation or indirectly by acting as cloud condensation nuclei (CCN) or ice nuclei (IN) in marine air (Murphy et al., 1998; Pierce and Adams, 2006; Hu et al., 2005; Kanji et al., 2017; Kong et al., 2018).

It is well known that the interaction of the continental-marine air masses not only releases some active substances into marine air but also supplies many nutrients (e.g., Fe, N, and P) for biological growth (e.g., plankton) to the ocean’s surface (Li et al.,

2017; Shi et al., 2012). Some studies have reported that the continental anthropogenic and natural pollutants can be carried to remote marine air through long-range atmospheric transport (Guo et al., 2014; Li et al., 2017; Moffet et al., 2012; Uematsu et al., 2010). The continental pollutants that are deposited into the ocean increase the nutrient input to the seawater, and finally alter the primary productivity in the open sea (Mahowald et al., 2018; Fu et al., 2018; Luo et al., 2016; Shi et al., 2012). Moreover, previous studies found that large amounts of light-absorbing aerosols (e.g., black carbon and brown carbon) from continental polluted air can be transported into the open ocean air and significantly influence the radiative balance of the marine boundary layer (Ueda et al., 2018; Kang et al., 2018; Zhang et al., 2014; Kondo et al., 2016). Therefore, it is important to understand the physicochemical properties of long-range transported anthropogenic aerosol particles in marine air.

The eastern China seas (ECS: the Yellow Sea and the East China Sea) and the northwestern Pacific Ocean (NWPO) can be affected by the Asian continental air masses under the prevailing westerly winds in winter and spring (Uematsu et al., 2010; Uno et al., 2009). At present, there have been many in-depth studies on the physicochemical properties of aerosols in air masses before they leave the Asian continent. For example, Li et al. (2014) collected aerosol particles at a background site in the Yellow River Delta and determined their physicochemical properties before leaving the Asian continent. Feng et al. (2012) studied the sources and formation pathways of $PM_{2.5}$ at Changdao Island, a resort island in Bohai Sea/Yellow Sea, which is in the transport path of the Asian continental outflow to the Pacific

Ocean. Shi et al. (2019) investigated aerosol particles from Asian continental outflow in Qingdao and found the solubility of phosphorus was related to the sources and atmospheric acidification processes. However, these atmospheric field observations were limited to some isolated continental sites.

Shipboard observations are an effective way to study marine aerosol properties in remote areas. Using the single particle analysis method (i.e., electron microscope), previous shipboard atmospheric studies have observed chloride depletion and sulfur enrichment in SSA particles from the marine boundary layer (McInnes et al., 1994; Mouri and Okada, 1993; Bondy et al., 2017). At a coastal city in southwestern Japan, Zhang et al. (2003) found that dust particles from Asian continent could mix with SSA particles in the marine atmosphere and further restrained chloride depletion from the sea-salt component in the particles. However, these studies did not examine how anthropogenic pollutants influence the physicochemical properties of SSA from the margin sea air to the remote marine air. Furthermore, they cannot continuously trace the changes of anthropogenic aerosol particles along the pollutants' transport path to the remote NWPO.

In this study, the research ship R/V Dongfanghong 2 was designed to cruise from the ECS to the NWPO so that we could understand what and how air pollutants are transported from the highly polluted continental air to clean marine air in spring. After the cruise, a transmission electron microscope was used to obtain composition, size, morphology, and mixing states of marine aerosol particles. Based on this information, we compared aerosol characteristics over the ECS and the remote NWPO.

Furthermore, we also discussed how the continental air masses influence marine aerosols in the ECS and the NWPO air.

2. Experiments

2.1 Aerosol sampling and analyses

Aerosol samples were collected on board the R/V Dongfanghong 2 during the cruise from 17 March to 22 April, 2014. The cruise path crossed the ECS and the NWPO (Figure 1). Aerosol particles were sampled onto copper TEM grids (carbon type-B, 300-mesh copper; Tianld Co., China) using a DKL-2 sampler (Genstar Electronic Technology, China). The sampler was equipped with a single-stage impactor with a 0.5 mm diameter jet nozzle at an airflow of 1.0 L/min. If the particle density is 2 g cm^{-3}, the collection efficiency of the sampler is 50% for particles with a 260 nm aerodynamic diameter. All the samples were collected at the ship's bow to avoid contamination from the exhaust. During the same cruise, the short-period contribution from contamination of particulate matter was less than 3% (Luo et al., 2016). The sampling duration varied from 2 to 3 min to avoid individual particles overlap on the substrate. After the collection, all the samples were sealed in dry plastic capsules and stored in a desiccator at 25 ℃ and 20 ± 3% relative humidity (RH) for further analysis.

The aerosol particles were analyzed by a JEOL JEM-2100 transmission electron microscope (TEM) operated at 200 kV. The chemical elements (heavier than carbon, $Z \geq 6$) were semi-quantitatively detected by an energy-dispersive X-ray spectrometer

(EDS) (Oxford Instruments, UK). Coarser particles are near the center of the sampling spot and finer particles are on the periphery. Therefore, we selected three or four areas from the center to the edge to guarantee the representativeness of the analyzed particles. The iTEM software (Olympus Soft Imaging Solutions GmbH, Germany) was used to analyze individual particles in the TEM images and obtain their projected area, perimeter, aspect ratio, and equivalent circle diameter (ECD).

A total of 22 samples were analyzed in this study. The location of each sample is shown in Figure 1. The details about sampling dates, times, and meteorological conditions for each sample are listed in Table S1. Due to the influence of the westerlies, the ECS is frequently affected by the air pollutants' transport from Asian spring (Shi et al., 2019). The NWPO is less affected by the transport of continental pollutants because of the remote distance (Zhang et al., 2018). According to the sample locations, we defined two sample categories along with the cruise path (Figure 1): 11 samples in the ECS and 11 samples in the NWPO.

2.2 Air mass backward trajectories

The NOAA HYSPLIT (Hybrid Single Particle Lagrangian Integrated Trajectory) trajectory model (Stein et al., 2015) was applied to calculate the backward trajectories for the investigation of air mass sources and transport paths. The total run time was set at 48 hours. We selected an altitude of 500 m as the endpoint in each backward trajectory. In this study, we obtained 21 backward trajectories.

3. Results

3.1 Classification and relative abundance of aerosol particles

The TEM analyses provided the morphology, mixing state, and composition of individual particles. In this study, we analyzed 3,734 particles in 22 samples (2,770 particles collected in the ECS and 964 particles in the NWPO). Aerosol particles were classified into seven types based on their composition and morphology: sulfur-rich (S-rich), organic matter (OM), soot, metal, fly ash, mineral, and sea salt. S-rich particles are considered as secondary inorganic particles (e.g., $(NH_4)_2SO_4$ and NH_4NO_3), which are formed from their gaseous precursors, such as SO_2, NO_x, and NH_3. OM particles mainly contain C and certain O and Si. Here we observed two kinds of OM particles: spherical or irregular primary organic matter (POM) particles and secondary organic matter (SOM) particles. The POM particles are directly emitted from the combustion of fossil fuel and biomass and SOM particles are formed from volatile organic compounds (VOCs) or the oxidized POM in the atmosphere (Li et al., 2016a; Wang et al., 2021). In the TEM images, the POM particles normally have a spherical or irregular shape. The SOM particles display a core-shell structure, which usually represents an inorganic core (e.g., sulfate) coated by secondary organics (Li et al., 2016b). Soot particles (i.e., black carbon) are chain-like aggregates of carbonaceous spheres, mainly containing C and minor O. Metal particles mainly contain Fe, Zn, and Pb, and fly ash particles contain Si, Al, and minor Ca and Fe. Metal and fly ash particles both display spherical shapes and are directly emitted from heavy industrial activities such as power plants and steel factories (Li et al., 2017). Mineral particles are composed of Si, Al, Ca, and Fe and present irregular shapes

(Figure 2a). Mineral particles originate from arid deserts (e.g., Sahara and Gobi), roads, and construction activities in the continental areas. Sea salt aerosol (SSA, Figure 2b) is from the bursting of air bubbles resulting from the waves breaking. SSA is mainly composed of Na and Cl, with minor Mg, Ca, K, and S.

The high-resolution TEM could see through the thin materials on the substrate, so the inner mixing structure of different aerosol components in individual particles can be directly identified (Li et al., 2016b; Riemer et al., 2019). We found that most of the individual non-SSA particles collected in marine air contained two or more different types of anthropogenic aerosols. To elucidate the mixing structure of the non-SSA particles, we further defined six types of internally mixed particles: S-metal, metal particles mixed with sulfate (Figure 2c); S-fly ash, fly ash particles mixed with sulfate (Figure 2d); S-soot, soot particles mixed with sulfate (Figure 2e); OM coating, SOM coated on sulfate (Figure 2f); OM-S, POM particle mixed with sulfate (Figure 2g); and S-rich, secondary inorganic sulfate and nitrate particles (e.g., $(NH_4)_2SO_4$ and NH_4NO_3) (Figure 2h). Anthropogenic aerosols are particles originated from human activities, including S-rich, S-soot, S-metal/fly ash, OM-S, and OM coating particles in this study. In the ECS, anthropogenic aerosols accounted for 87% of all particles by number fraction, including S-rich for 42 %, S-soot for 21%, S-metal/fly ash for 8%, OM-S for 6%, and OM coating for 10%. Only 8% of the observed particles in the ECS were SSA particles. The remaining 5% was identified as mineral particles. Interestingly, SSA particles became the dominant aerosol at 90% in the NWPO and anthropogenic aerosols only accounted for 8%, suggesting that marine emissions

194 became the major aerosol source in the NWPO. Therefore, there are large differences
195 between aerosol particles in the ECS and the NWPO (Figure 3).
196
197 **3.2 Variations of aerosol particles from the ECS to the NWPO**
198 Figure 3 shows variations of aerosol particles along with the cruise pathway from
199 the ECS to the NWPO. Mineral particles can only be transported from continental
200 areas. Figure 3 shows that higher number fractions of mineral particles always
201 occurred when the sampling sites were close to eastern China. The number fraction of
202 mineral particles rose to 15% in the coastal air during the cruise (Figure 3). The
203 proportion of mineral particles decreased from 15% to 3% for the samples collected in
204 the ECS. When the ship traveled eastward into the NWPO, the proportion of mineral
205 particles dropped to a low level (2%). In contrast, the proportion of mineral particles
206 increased again when the ship returned to the ECS. Altogether, the number fraction of
207 mineral particles was 5% in the ECS, higher than that in the NWPO, suggesting that
208 the ECS and NWPO were influenced by westerlies during the sampling period. Indeed,
209 Figure 1 shows that most of 48h backward trajectories of air masses in the ECS were
210 sourced from eastern China and that some of the 48h back trajectories of air masses in
211 the NWPO crossed Japan.
212 Figure 3 shows that S-metal and S-fly ash (two typical anthropogenic aerosol
213 particles) displayed variation similar to the mineral particles. Number fractions of
214 S-metal and S-fly ash particles in the ECS samples ranged from 17% to 2% with the
215 average value at 8%, but only 0.3% for S-metal and S-fly ash particle was found in

the NWPO. In a word, we conclude that aerosol particles from the Asian continent directly exert much greater impacts on the ECS than the NWPO.

3.3 Comparison of anthropogenic secondary aerosol particles

Secondary S-rich and OM coating particles are normally considered as arising from the conversion of anthropogenic gaseous pollutants (e.g., SO_2, NO_x, NH_3, and VOCs) (Li et al., 2021). TEM observations clearly identified secondary particles and showed their variation of number fraction in the samples (Figure 3). Our results show that number fractions of S-rich particles were dominant in the ECS samples with the range of 32%-71%, but their fractions decreased to 5% in the NWPO. The results indicate that secondary particles in the ECS were strongly influenced by anthropogenic pollutants transported from eastern China. Furthermore, we noticed that secondary aerosol particles were frequently mixed with some typical fine primary anthropogenic particles (e.g., soot, fly ash, and metal) and formed S-soot/S-fly ash/S-metal particles (Figure 4). As a result, we conclude that the anthropogenic gases or aerosol pollutants in the continental air masses significantly influence the downwind air quality of the ECS, but they have a minor impact on the NWPO air.

It should be noted that OM coating particles were frequently found in the ECS but barely observed in the NWPO. In other words, S-rich particles in the NWPO had no typical OM coating, although S-rich particles accounted for ~5% in the NWPO samples. Figure 4b shows that these S-rich particles in the NWPO only had one dominant size range smaller than 1 μm, which is different from the larger and broader size distribution of S-rich particles in the ECS. In addition, we noticed the particularly

high fraction of S-rich particles in Sample #11 and #12 collected in the NWPO (15% and 24%). Coincidently, Zhu et al. (2019) observed a new particle formation event in the same area and proposed that the event was likely caused by long-range transported continental gases (e.g., SO_2, NO_x, and VOCs).

3.4 Aging of sea salt aerosols

As the dominant aerosol particles in marine air, SSA particles accounted for 70%-98% in the NWPO. SSA could serve as reactive surfaces for heterogeneous and multiphase chemical reactions in the atmosphere, and these reactions also could alter the morphology and composition of SSA (Athanasopoulou et al., 2008; Chi et al., 2015; Laskin et al., 2012). Based on the morphology and composition of SSA, we further classified SSA into three categories: fresh SSA, partially aged SSA, and fully aged SSA (Figure 5).

The fresh SSA did not experience any chemical modification in the atmosphere. TEM images of fresh SSA indicate the cubic NaCl core and coating composed of $MgCl_2$ and $CaSO_4$ (Figure 5a). The NaCl core only contains Na and Cl, with the atomic ratio of Na to Cl close to 1:1 (Figure 5d). The major components in the coating are Mg, O, S, Cl, and Ca (Figure 5e), thus, we infer their molecular forms as $MgCl_2$ and $CaSO_4$ (Geng et al., 2010; Chi et al., 2015; Pósfai et al., 1994; Buseck and Pósfai, 1999).

The partially aged SSA represent those SSA particles that undergo chemical modification but still retain part of the NaCl core (Figure 5b). The morphological differences can be observed between the fresh SSA and partially aged SSA. The NaCl

core still persists in the partially aged SSA but cannot keep its regular cubic shape. Meanwhile, the coating composition turns into O, Na, Mg, Ca, and S, with decreasing Cl (Figure 5f). The SSA aging is attributed to the Cl-depletion phenomena, which can be expressed as follows (Laskin et al., 2012):

$$NaCl\ (aq) + HA\ (aq, g) \rightarrow NaA\ (aq) + HCl\ (aq, g)$$

where HA represents atmospheric acids (e.g., H_2SO_4, HNO_3, and methanesulfonic acid). NaCl in the SSA could react with inorganic (e.g., HNO_3 and H_2SO_4) or organic acid (e.g., methanesulfonic acid), releasing volatile HCl (g) to the atmosphere, leading to depletion in chloride and enrichment in corresponding sodium salts.

We define the fully aged SSA as particles whose NaCl cores have been completely transformed into $NaNO_3$ and Na_2SO_4. Figure 5c shows that the NaCl cores in the fully aged SSA entirely disappeared, leaving a rounder shape. The Cl element was no longer detected in the fully aged SSA and the major aerosol components were the mixture of $NaNO_3$ and Na_2SO_4 (Figure 5g).

To evaluate composition differences of SSA, we present triangular diagrams of Na-Cl-S weight ratio based on the EDS. Figure 6a shows that the fresh SSA is around the NaCl, the partially aged SSA is distributed in the center of triangular, and the fully aged SSA is around $NaNO_3$ and Na_2SO_4. Figure 6b shows that there were large variations of the SSA components in the ECS and NWPO. Our results show that most of the aged SSA in the ECS were the mixture of $NaNO_3$ and Na_2SO_4, suggesting that SSA in the ECS underwent heterogeneous reactions and become fully aged SSA. SSA in the NWPO is widely distributed between NaCl and $NaNO_3$/Na_2SO_4 in the

triangular diagram, suggesting that these were partially aged SSA particles.

Figure 7 shows the relative abundance of SSA at different sampling sites from the ECS to the NWPO. In the ECS, 87% of SSA particles were fully aged. As the ship traveled into the NWPO, fully aged SSA particles decreased to 29%, meanwhile the proportion of fresh SSA increased to 57%. The size distribution of SSA particles shows that the proportion of fresh SSA increased with the increase of particle size from 0.05 to 5 μm (Figure 8). On the contrary, the proportion of fully aged SSA decreased with the increase of particle size from 0.05 to 5 μm. Overall, partially and fully aged SSA accounted for 61% of SSA particles smaller than 3 μm, while fresh SSA dominated (81%) in SSA particles larger than 3 μm. Figure 8 also reveals that 94% of the fully aged SSA particles were smaller than 3 μm.

4. Discussion

Abundant BC, metal, and fly ash particles in the ECS show that long-range transport of anthropogenic aerosol particles from the polluted continental air constantly influence the ECS air during the spring and winter. Moreover, the existence of OM coating particles (10%, Figure 3) in the ECS indicates that secondary sulfate/nitrate particles underwent aging process and formed the OM coating during their transport (Li et al., 2021). This result suggests that the long-range transported air masses from continental areas brought abundant anthropogenic gases such as NO_x, SO_2, and VOCs into marine air. Indeed, the HYSPLIT backward trajectories show that the air masses in the ECS samples were mainly from eastern China (Figure 1).

Under the influence of the westerlies, a large number of anthropogenic and natural pollutants are transported to the ECS and further influence its air quality. Most of air masses in the NWPO samples originated from northwest, passing through Japan to sampling location within 48 hours.

Figure 3 shows that anthropogenic aerosols were relatively low in the NWPO (8%), suggesting a slight influence from continental aerosols. However, we observed severe Cl-depletion in SSA in some samples in the NWPO. The Cl-depletion of SSA is mainly caused by the heterogeneous reactions with acidic gaseous pollutants in marine air (Hsu et al., 2007; Chi et al., 2015; Laskin et al., 2012). By comparing the aging degree of SSA and air mass backward trajectories, we found that the air masses with a relatively high proportion of fully aged SSA particles (#13 and #15) mostly formed due to the anthropogenic gaseous pollutants (e.g., SO_2 and NO_x) from northwest China and Japan (Figure S1). The result suggests that aerosol particles and gases might have different transport distances. Aerosol particles could be significantly removed by dry or wet deposition. However, the anthropogenic gases can be transported further to the NWPO air. Over the western Pacific, Koike et al. (2003) also found that anthropogenic gaseous pollutants (e.g., NO_x and SO_2) from the East Asia have higher transport efficiency than aerosols from the same region. Meanwhile, the surface changes of SSA can be considered as a potential indicator for anthropogenic gaseous pollutants in remote marine air.

Based on the results and discussion above, a conceptual model was proposed to summarize the impact of long-range transported anthropogenic air pollutants on

marine aerosols. Both anthropogenic gases and aerosol particles could be transported to the downwind marine air. Anthropogenic aerosol particles from the continent significantly influence the ECS air. During the transport, aerosol particles could be scavenged due to dry or wet deposition while some reactive gases can be transported further to the NWPO air and influence the aging of SSA particles.

Figure 6 shows a higher percentage of Cl-free SSA particles (on Cl = 0 line) in the ECS than those in NWPO, suggesting modifications of SSA in the ECS were much more severe than them in the NWPO. Referred to Zhang et al. (2003), we further provide the dash line that Na:Cl:S was changed only by reaction with H_2SO_4. Thus, particles above the dash line represent that Cl in these SSA particles was not only replaced by S deposition, other chemical processes (e.g., react with HNO_3 and organic acids) also contributed to the Cl-depletion. The number of fully aged SSA particles above the dash line was further counted. For the fully aged SSA particles, 70% of them in the ECS were above the dash line, while the proportion increased to 86% in the NWPO (Figure 6). The result indicates that S deposition could not compensate for Cl-depletion in most of the fully aged SSA particles in both ECS and NWPO. There must be other acids leading to Cl-depletion in the fully aged SSA particles besides the reaction with H_2SO_4.

It is well known that organic acids could also be a reason of Cl-depletion in SSA (Laskin et al., 2012; Chi et al., 2015; Ghorai et al., 2014). The oxidation of dimethyl sulfide (DMS) emitted from phytoplankton contributes to the Cl-depletion in SSA (Sievering et al., 2004). Both anthropogenic acidic gases and DMS in the ECS were

348 found to be higher than that in the NWPO (Figures S1 and S2). Compared with the
349 ECS, we found that DMS in our NWPO shipping area had lower mass concentrations
350 and minor fluctuations (3-6 $\times 10^{-11}$ kg m^3, Fig S2). However, the percentages of aged
351 SSA differed widely (from 23% to 88%) within the NWPO. We deduce that the low
352 concentration of the DMS only slightly modified part of SSA in the NWPO, but it was
353 not enough to influence all the SSA. Moreover, Zhu et al. (2019) reported that
354 secondary sulfate particles in the NWPO were mostly came from the long-range
355 transported acidic gases during the sampling period. The contribution of DMS to
356 non-sea-salt sulfate is less than 6% in the remote ocean of the northern hemisphere
357 (Quinn et al., 1990; Savoie et al., 1994; George et al., 2008). Therefore, a large
358 proportion of aged SSA particles in the NWPO should be mainly attributed to the
359 anthropogenic acidic gases from long-range transport.

360 Meteorological conditions also play an important role in SSA particles aging. The
361 hygroscopic cycle of the pure SSA particles shows the deliquescence relative
362 humidity (DRH) near 75% and its efflorescence relative humidity (ERH) near 44%.
363 However, the natural SSA particles begin to take up water at 57% and form a liquid
364 layer on particles due to various inorganic compounds (e.g., $MgSO_4$, $MgCl_2$, and
365 $CaCl_2$) (Wise et al., 2009). In our study, the sampling RH values were higher than 40%
366 and more than half of them were collected at RH above 60% (Table S1). Therefore,
367 most SSA particles should exist as aqueous droplets during the particle hygroscopic
368 cycle, or at least particle surfaces kept the aqueous phase due to the existence of
369 various inorganic compounds (Wise et al., 2009). One previous study showed that

Cl-depletion in the aqueous SSA particles due to ozone under UV can produce Cl_2 (Oum et al., 1998). However, the averaged ozone concentration ranging from 42 to 50 ppb during our cruise did not exhibit large differences from the satellite observation in marine air (Figure S1c). Therefore, we conclude that ozone might be one factor causing Cl-depletion in aqueous SSA particles but should not be the major reason leading to the variations of SSA aging degree in different NWPO samples.

Previous studies found that SSA emissions increased with the increase of wind speed (Shinozuka et al., 2004; Pant et al., 2008; Feng et al., 2017). In our study, the proportion of fresh SSA increases with increasing wind speed (Figure 7), consistent with the aforementioned studies. SSA particle with a smaller size has lower dry deposition velocity and longer lifetime in the air (Lewis and Schwartz, 2004), which could enhance the Cl-depletion due to inorganic or organic acids. This could be the reason that partially and fully aged SSA particles were mostly in the smaller size range (<3 μm) (Figure 8). On the contrary, the newly emitted coarse SSA particles with high dry deposition velocity are more likely to deposit to the ocean, resulting in less reacted SSA. As a result, the fresh SSA from local sea spray was mostly found in the coarse size range (larger than 3 μm) in our samples (Figure 8). This result suggests that it is crucial to study aging process among the size-resolved SSA, especially particles smaller than 3 μm.

In the future, we need to pay more attention to the influence of anthropogenic gaseous pollutants on the SSA aging in remote marine air. On the one hand, the aging processes could modify the hygroscopicity of SSA, determining their morphology and

phase state in the humidified marine environment, in the end directly affecting optical properties of SSA (Wang et al., 2019). On the other hand, the hygroscopicity change due to SSA aging could alter CCN activity, and indirectly affect global climate (Murphy et al., 1998; Pierce and Adams, 2006; Hu et al., 2005). Meanwhile, the SSA also serves as an important sink for the anthropogenic acidic gases in remote marine areas (Chi et al., 2015; Laskin et al., 2012). Thus, in future research, it would be crucial to quantify the anthropogenic acidic gases scavenged by SSA.

5. Conclusions

Individual aerosol particles were collected from 17 March to 22 April, 2014 on board of the ship R/V Dongfanghong 2 from the ECS to the NWPO. We classified aerosol particles based on their composition, morphology, and mixing state: mineral, sea salt, S-metal, S-fly ash, S-soot, OM coating, OM-S, and S-rich. Microscopic analysis showed that anthropogenic aerosols accounted for 87% of the total particle number in the ECS. In particular, higher proportions of secondary particles (i.e., S-rich particles, 42%, and OM coating particles, 10%) were found in the ECS. Meanwhile, anthropogenic aerosols are relatively low in the NWPO (8%).

TEM observations revealed that SSA particles were the most abundant in the NWPO atmosphere, accounting for 90% of all analyzed aerosol particles. The Cl-depletion of sea salt aerosol (SSA) particles caused by the heterogeneous reactions with acidic gaseous pollutants was further observed. Three types of SSA particles, fresh, partially aged, and fully aged were classified. Fully aged SSA particles were the

dominant SSA in the ECS (87%), while fully aged SSA particles decreased to 29% in the NWPO. The severe aging of SSA (partially and fully aged, at most 88% of SSA) was still found in the NWPO, despite there being only minor anthropogenic aerosol particles. These results show that aerosol particles from the continent air might be removed by dry and wet deposition, but the air pollutants were transported further to the NWPO. The aging of SSA particles has important effects on their hygroscopic and optical properties, one effect being the promotion of heterogeneous reaction with acidic gases in the NWPO. Our observations show that more attention should be given to the influence of anthropogenic gaseous pollutants on the Cl-depletion on SSA in remote marine air.

Supplement

The supplement related to this article is available online at:

Author contributions

LX and WL conceived the study and wrote the article. The sampling during the research cruise was organized by XL, HG, and XY. LX, WL, LL, JZ, YZ, YW, and QY carried out TEM analyses of individual particles. DZ and LB contributed to the improvement of this paper. All authors reviewed and approved the paper.

Competing interests

The authors declare that they have no conflict of interest.

Acknowledgements

We thank Peter Hyde for his editorial comments. We acknowledge the NOAA Air Resources Laboratory for the provision of the HYSPLIT transport and dispersion model and READY website (http://www.ready.noaa.gov) used in this publication.

Financial support

This research was supported by the National Natural Science Foundation of China (grant nos. 42075096, 91844301, and 41805099), the National Key R&D Program of China (grant no. 2017YFC0212700), Zhejiang Provincial Natural Science Foundation of China (grant no. LZ19D050001), and China Postdoctoral Science Foundation (grant no. 2019M662021).

References

Athanasopoulou, E., Tombrou, M., Pandis, S. N., and Russell, A. G.: The role of sea-salt emissions and heterogeneous chemistry in the air quality of polluted coastal areas, Atmos. Chem. Phys., 8, 5755-5769, https://doi.org/10.5194/acp-8-5755-2008, 2008.

Bondy, A. L., Wang, B., Laskin, A., Craig, R. L., Nhliziyo, M. V., Bertman, S. B., Pratt, K. A., Shepson, P. B., and Ault, A. P.: Inland Sea Spray Aerosol Transport and Incomplete Chloride Depletion: Varying Degrees of Reactive Processing Observed during SOAS, Environ. Sci. Technol., 51, 9533-9542, https://doi.org/10.1021/acs.est.7b02085, 2017.

Buseck, P. R., and Pósfai, M.: Airborne minerals and related aerosol particles: Effects on climate and the environment, Proc. Natl. Acad. Sci. U.S.A., 96, 3372-3379, https://doi.org/10.1073/pnas.96.7.3372, 1999.

Chi, J. W., Li, W. J., Zhang, D. Z., Zhang, J. C., Lin, Y. T., Shen, X. J., Sun, J. Y., Chen, J. M., Zhang, X. Y., Zhang, Y. M., and Wang, W. X.: Sea salt aerosols as a reactive surface for inorganic and organic acidic gases in the Arctic troposphere, Atmos. Chem. Phys., 15, 11341-11353, https://doi.org/10.5194/acp-15-11341-2015, 2015.

Cravigan, L. T., Mallet, M. D., Vaattovaara, P., Harvey, M. J., Law, C. S., Modini, R. L., Russell, L. M., Stelcer, E., Cohen, D. D., Olsen, G., Safi, K., Burrell, T. J., and Ristovski, Z.: Sea spray aerosol

organic enrichment, water uptake and surface tension effects, Atmos. Chem. Phys., 20, 7955-7977, https://doi.org/10.5194/acp-20-7955-2020, 2020.

Feng, J. L., Guo, Z. G., Zhang, T. R., Yao, X. H., Chan, C. K., and Fang, M.: Source and formation of secondary particulate matter in $PM_{2.5}$ in Asian continental outflow, J. Geophys. Res.: Atmos., 117, D03302, https://doi.org/10.1029/2011jd016400, 2012.

Feng, L., Shen, H., Zhu, Y., Gao, H., and Yao, X.: Insight into Generation and Evolution of Sea-Salt Aerosols from Field Measurements in Diversified Marine and Coastal Atmospheres, Sci. Rep., 7, 41260, https://doi.org/10.1038/srep41260, 2017.

Fu, J., Wang, B., Chen, Y., and Ma, Q.: The influence of continental air masses on the aerosols and nutrients deposition over the western North Pacific, Atmos. Environ., 172, 1-11, https://doi.org/10.1016/j.atmosenv.2017.10.041, 2018.

Geng, H., Ryu, J., Jung, H.-J., Chung, H., Ahn, K.-H., and Ro, C.-U.: Single-Particle Characterization of Summertime Arctic Aerosols Collected at Ny-Ålesund, Svalbard, Environ. Sci. Technol., 44, 2348-2353, https://doi.org/10.1021/es903268j, 2010.

George, S. K., Nair, P. R., Parameswaran, K., Jacob, S., and Abraham, A.: Seasonal trends in chemical composition of aerosols at a tropical coastal site of India, J. Geophys. Res.: Atmos., 113, D16209, https://doi.org/10.1029/2007JD009507, 2008.

Ghorai, S., Wang, B., Tivanski, A., and Laskin, A.: Hygroscopic Properties of Internally Mixed Particles Composed of NaCl and Water-Soluble Organic Acids, Environ. Sci. Technol., 48, 2234-2241, https://doi.org/10.1021/es404727u, 2014.

Guo, L., Chen, Y., Wang, F., Meng, X., Xu, Z., and Zhuang, G.: Effects of Asian dust on the atmospheric input of trace elements to the East China Sea, Mar. Chem., 163, 19-27, https://doi.org/10.1016/j.marchem.2014.04.003, 2014.

Hsu, S.-C., Liu, S. C., Kao, S.-J., Jeng, W.-L., Huang, Y.-T., Tseng, C.-M., Tsai, F., Tu, J.-Y., and Yang, Y.: Water-soluble species in the marine aerosol from the northern South China Sea: High chloride depletion related to air pollution, J. Geophys. Res.: Atmos., 112, D19304, https://doi.org/10.1029/2007JD008844, 2007.

Hu, R. M., Blanchet, J. P., and Girard, E.: Evaluation of the direct and indirect radiative and climate effects of aerosols over the western Arctic, J. Geophys. Res.: Atmos., 110, D11213, https://doi.org/10.1029/2004JD005043, 2005.

Kang, M., Fu, P., Kawamura, K., Yang, F., Zhang, H., Zang, Z., Ren, H., Ren, L., Zhao, Y., Sun, Y., and Wang, Z.: Characterization of biogenic primary and secondary organic aerosols in the marine atmosphere over the East China Sea, Atmos. Chem. Phys., 18, 13947-13967, https://doi.org/10.5194/acp-18-13947-2018, 2018.

Kanji, Z. A., Ladino, L. A., Wex, H., Boose, Y., Burkert-Kohn, M., Cziczo, D. J., and Krämer, M.: Overview of Ice Nucleating Particles, Meteorological Monographs, 58, 1.1-1.33, https://doi.org/10.1175/amsmonographs-d-16-0006.1, 2017.

Koike, M., Kondo, Y., Kita, K., Takegawa, N., Masui, Y., Miyazaki, Y., Ko, M. W., Weinheimer, A. J., Flocke, F., Weber, R. J., Thornton, D. C., Sachse, G. W., Vay, S. A., Blake, D. R., Streets, D. G., Eisele, F. L., Sandholm, S. T., Singh, H. B., and Talbot, R. W.: Export of anthropogenic reactive nitrogen and sulfur compounds from the East Asia region in spring, J. Geophys. Res.: Atmos., 108, 8789, https://doi.org/10.1029/2002JD003284, 2003.

Kondo, Y., Moteki, N., Oshima, N., Ohata, S., Koike, M., Shibano, Y., Takegawa, N., and Kita, K.: Effects of wet deposition on the abundance and size distribution of black carbon in East Asia, J.

Geophys. Res.: Atmos., 121, 4691-4712, https://doi.org/10.1002/2015JD024479, 2016.
Kong, X., Wolf, M. J., Roesch, M., Thomson, E. S., Bartels-Rausch, T., Alpert, P. A., Ammann, M., Prisle, N. L., and Cziczo, D. J.: A continuous flow diffusion chamber study of sea salt particles acting as cloud nuclei: deliquescence and ice nucleation, Tellus B: Chemical and Physical Meteorology, 70, 1-11, https://doi.org/10.1080/16000889.2018.1463806, 2018.
Laskin, A., Moffet, R. C., Gilles, M. K., Fast, J. D., Zaveri, R. A., Wang, B., Nigge, P., and Shutthanandan, J.: Tropospheric chemistry of internally mixed sea salt and organic particles: Surprising reactivity of NaCl with weak organic acids, J. Geophys. Res.: Atmos., 117, D15302, https://doi.org/10.1029/2012JD017743, 2012.
Lewis, E. R., and Schwartz, S. E.: Sea salt aerosol production: mechanisms, methods, measurements, and models, American Geophysical Union, Washington, DC, U.S.A, 2004.
Li, W., Shao, L., Shi, Z., Chen, J., Yang, L., Yuan, Q., Yan, C., Zhang, X., Wang, Y., Sun, J., Zhang, Y., Shen, X., Wang, Z., and Wang, W.: Mixing state and hygroscopicity of dust and haze particles before leaving Asian continent, J. Geophys. Res.: Atmos., 119, 1044-1059, https://doi.org/10.1002/2013JD021003, 2014.
Li, W., Shao, L., Zhang, D., Ro, C.-U., Hu, M., Bi, X., Geng, H., Matsuki, A., Niu, H., and Chen, J.: A review of single aerosol particle studies in the atmosphere of East Asia: morphology, mixing state, source, and heterogeneous reactions, J. Clean. Prod., 112, Part 2, 1330-1349, https://doi.org/10.1016/j.jclepro.2015.04.050, 2016a.
Li, W., Sun, J., Xu, L., Shi, Z., Riemer, N., Sun, Y., Fu, P., Zhang, J., Lin, Y., Wang, X., Shao, L., Chen, J., Zhang, X., Wang, Z., and Wang, W.: A conceptual framework for mixing structures in individual aerosol particles, J. Geophys. Res.: Atmos., 121, 13784-13798, https://doi.org/10.1002/2016JD025252, 2016b.
Li, W., Xu, L., Liu, X., Zhang, J., Lin, Y., Yao, X., Gao, H., Zhang, D., Chen, J., Wang, W., Harrison, R. M., Zhang, X., Shao, L., Fu, P., Nenes, A., and Shi, Z.: Air pollution–aerosol interactions produce more bioavailable iron for ocean ecosystems, Sci. Adv., 3, e1601749, https://doi.org/10.1126/sciadv.1601749, 2017.
Li, W., Liu, L., Zhang, J., Xu, L., Wang, Y., Sun, Y., and Shi, Z.: Microscopic Evidence for Phase Separation of Organic Species and Inorganic Salts in Fine Ambient Aerosol Particles, Environ. Sci. Technol., 55, 2234-2242, https://doi.org/10.1021/acs.est.0c02333, 2021.
Luo, L., Yao, X. H., Gao, H. W., Hsu, S. C., Li, J. W., and Kao, S. J.: Nitrogen speciation in various types of aerosols in spring over the northwestern Pacific Ocean, Atmos. Chem. Phys., 16, 325-341, https://doi.org/10.5194/acp-16-325-2016, 2016.
Mahowald, N. M., Hamilton, D. S., Mackey, K. R. M., Moore, J. K., Baker, A. R., Scanza, R. A., and Zhang, Y.: Aerosol trace metal leaching and impacts on marine microorganisms, Nat. Commun., 9, 2614, https://doi.org/10.1038/s41467-018-04970-7, 2018.
McInnes, L. M., Covert, D. S., Quinn, P. K., and Germani, M. S.: Measurements of chloride depletion and sulfur enrichment in individual sea-salt particles collected from the remote marine boundary layer, J. Geophys. Res.: Atmos., 99, 8257-8268, https://doi.org/10.1029/93JD03453, 1994.
Moffet, R. C., Furutani, H., Rödel, T. C., Henn, T. R., Sprau, P. O., Laskin, A., Uematsu, M., and Gilles, M. K.: Iron speciation and mixing in single aerosol particles from the Asian continental outflow, J. Geophys. Res.: Atmos., 117, D07204, https://doi.org/10.1029/2011JD016746, 2012.
Mouri, H., and Okada, K.: Shattering and modification of sea-salt particles in the marine atmosphere, Geophys. Res. Lett., 20, 49-52, https://doi.org/10.1029/92GL03004, 1993.

554 Murphy, D., Anderson, J., Quinn, P., McInnes, L., Brechtel, F., Kreidenweis, S., Middlebrook, A.,
555 Pósfai, M., Thomson, D., and Buseck, P.: Influence of sea-salt on aerosol radiative properties in the
556 Southern Ocean marine boundary layer, Nature, 392, 62-65, https://doi.org/10.1038/32138, 1998.
557 O'Dowd Colin, D., and de Leeuw, G.: Marine aerosol production: a review of the current knowledge,
558 Phil. Trans. R. Soc. A., 365, 1753-1774, https://doi.org/10.1098/rsta.2007.2043, 2007.
559 Oum, K. W., Lakin, M. J., DeHaan, D. O., Brauers, T., and Finlayson-Pitts, B. J.: Formation of
560 Molecular Chlorine from the Photolysis of Ozone and Aqueous Sea-Salt Particles, Science, 279,
561 74-76, https://doi.org/10.1126/science.279.5347.74, 1998.
562 Pósfai, M., Anderson, J. R., Buseck, P. R., Shattuck, T. W., and Tindale, N. W.: Constituents of a remote
563 pacific marine aerosol: A tem study, Atmos. Environ., 28, 1747-1756,
564 https://doi.org/10.1016/1352-2310(94)90137-6, 1994.
565 Pant, V., Deshpande, C. G., and Kamra, A. K.: On the aerosol number concentration–wind speed
566 relationship during a severe cyclonic storm over south Indian Ocean, J. Geophys. Res.: Atmos., 113,
567 D02206, https://doi.org/10.1029/2006JD008035, 2008.
568 Pierce, J. R., and Adams, P. J.: Global evaluation of CCN formation by direct emission of sea salt and
569 growth of ultrafine sea salt, J. Geophys. Res.: Atmos., 111, D06203,
570 https://doi.org/10.1029/2005JD006186, 2006.
571 Quinn, P. K., Bates, T. S., Johnson, J. E., Covert, D. S., and Charlson, R. J.: Interactions between the
572 sulfur and reduced nitrogen cycles over the central Pacific Ocean, J. Geophys. Res.: Atmos., 95,
573 16405-16416, https://doi.org/10.1029/JD095iD10p16405, 1990.
574 Riemer, N., Ault, A. P., West, M., Craig, R. L., and Curtis, J. H.: Aerosol Mixing State: Measurements,
575 Modeling, and Impacts, Rev. Geophys., 57, 187-249, https://doi.org/10.1029/2018rg000615, 2019.
576 Savoie, D. L., Prospero, J. M., Arimoto, R., and Duce, R. A.: Non-sea-salt sulfate and methanesulfonate
577 at American Samoa, J. Geophys. Res.: Atmos., 99, 3587-3596, https://doi.org/10.1029/93JD03337,
578 1994.
579 Shi, J., Wang, N., Gao, H., Baker, A. R., Yao, X., and Zhang, D.: Phosphorus solubility in aerosol
580 particles related to particle sources and atmospheric acidification in Asian continental outflow,
581 Atmos. Chem. Phys., 19, 847-860, https://doi.org/10.5194/acp-19-847-2019, 2019.
582 Shi, Z., Krom, M. D., Jickells, T. D., Bonneville, S., Carslaw, K. S., Mihalopoulos, N., Baker, A. R.,
583 and Benning, L. G.: Impacts on iron solubility in the mineral dust by processes in the source region
584 and the atmosphere: A review, Aeolian Research, 5, 21-42,
585 https://doi.org/10.1016/j.aeolia.2012.03.001, 2012.
586 Shinozuka, Y., Clarke, A. D., Howell, S. G., Kapustin, V. N., and Huebert, B. J.: Sea-salt vertical
587 profiles over the Southern and tropical Pacific oceans: Microphysics, optical properties, spatial
588 variability, and variations with wind speed, J. Geophys. Res.: Atmos., 109, D24201,
589 https://doi.org/10.1029/2004JD004975, 2004.
590 Sievering, H., Cainey, J., Harvey, M., McGregor, J., Nichol, S., and Quinn, P.: Aerosol non-sea-salt
591 sulfate in the remote marine boundary layer under clear-sky and normal cloudiness conditions:
592 Ocean-derived biogenic alkalinity enhances sea-salt sulfate production by ozone oxidation, J.
593 Geophys. Res.: Atmos., 109, D19317, https://doi.org/10.1029/2003JD004315, 2004.
594 Ueda, S., Osada, K., Hara, K., Yabuki, M., Hashihama, F., and Kanda, J.: Morphological features and
595 mixing states of soot-containing particles in the marine boundary layer over the Indian and Southern
596 oceans, Atmos. Chem. Phys., 18, 9207-9224, https://doi.org/10.5194/acp-18-9207-2018, 2018.
597 Uematsu, M., Hattori, H., Nakamura, T., Narita, Y., Jung, J., Matsumoto, K., Nakaguchi, Y., and Kumar,

M. D.: Atmospheric transport and deposition of anthropogenic substances from the Asia to the East China Sea, Mar. Chem., 120, 108-115, https://doi.org/10.1016/j.marchem.2010.01.004, 2010.

Uno, I., Eguchi, K., Yumimoto, K., Takemura, T., Shimizu, A., Uematsu, M., Liu, Z., Wang, Z., Hara, Y., and Sugimoto, N.: Asian dust transported one full circuit around the globe, Nat. Geosci., 2, 557-560, https://doi.org/10.1038/ngeo583, 2009.

Wang, J., Ye, J., Zhang, Q., Zhao, J., Wu, Y., Li, J., Liu, D., Li, W., Zhang, Y., Wu, C., Xie, C., Qin, Y., Lei, Y., Huang, X., Guo, J., Liu, P., Fu, P., Li, Y., Lee, H. C., Choi, H., Zhang, J., Liao, H., Chen, M., Sun, Y., Ge, X., Martin, S. T., and Jacob, D. J.: Aqueous production of secondary organic aerosol from fossil-fuel emissions in winter Beijing haze, Proc. Natl. Acad. Sci. U.S.A., 118, e2022179118, https://doi.org/10.1073/pnas.2022179118, 2021.

Wang, Z., Bi, L., Yi, B., and Zhang, X.: How the Inhomogeneity of Wet Sea Salt Aerosols Affects Direct Radiative Forcing, Geophys. Res. Lett., 46, 1805-1813, https://doi.org/10.1029/2018GL081193, 2019.

Wise, M. E., Freney, E. J., Tyree, C. A., Allen, J. O., Martin, S. T., Russell, L. M., and Buseck, P. R.: Hygroscopic behavior and liquid-layer composition of aerosol particles generated from natural and artificial seawater, J. Geophys. Res.: Atmos., 114, D03201, https://doi.org/10.1029/2008JD010449, 2009.

Yao, X., and Zhang, L.: Chemical processes in sea-salt chloride depletion observed at a Canadian rural coastal site, Atmos. Environ., 46, 189-194, https://doi.org/10.1016/j.atmosenv.2011.09.081, 2012.

Zhang, D., Iwasaka, Y., Shi, G., Zang, J., Matsuki, A., and Trochkine, D.: Mixture state and size of Asian dust particles collected at southwestern Japan in spring 2000, J. Geophys. Res.: Atmos., 108, 4760, https://doi.org/10.1029/2003JD003869, 2003.

Zhang, X., Massoli, P., Quinn, P. K., Bates, T. S., and Cappa, C. D.: Hygroscopic growth of submicron and supermicron aerosols in the marine boundary layer, J. Geophys. Res.: Atmos., 119, 8384-8399, https://doi.org/10.1002/2013JD021213, 2014.

Zhang, X. X., Sharratt, B., Liu, L. Y., Wang, Z. F., Pan, X. L., Lei, J. Q., Wu, S. X., Huang, S. Y., Guo, Y. H., Li, J., Tang, X., Yang, T., Tian, Y., Chen, X. S., Hao, J. Q., Zheng, H. T., Yang, Y. Y., and Lyu, Y. L.: East Asian dust storm in May 2017: observations, modelling, and its influence on the Asia-Pacific region, Atmos. Chem. Phys., 18, 8353-8371, https://doi.org/10.5194/acp-18-8353-2018, 2018.

Zhu, Y., Li, K., Shen, Y., Gao, Y., Liu, X., Yu, Y., Gao, H., and Yao, X.: New particle formation in the marine atmosphere during seven cruise campaigns, Atmos. Chem. Phys., 19, 89-113, https://doi.org/10.5194/acp-19-89-2019, 2019.

Figures

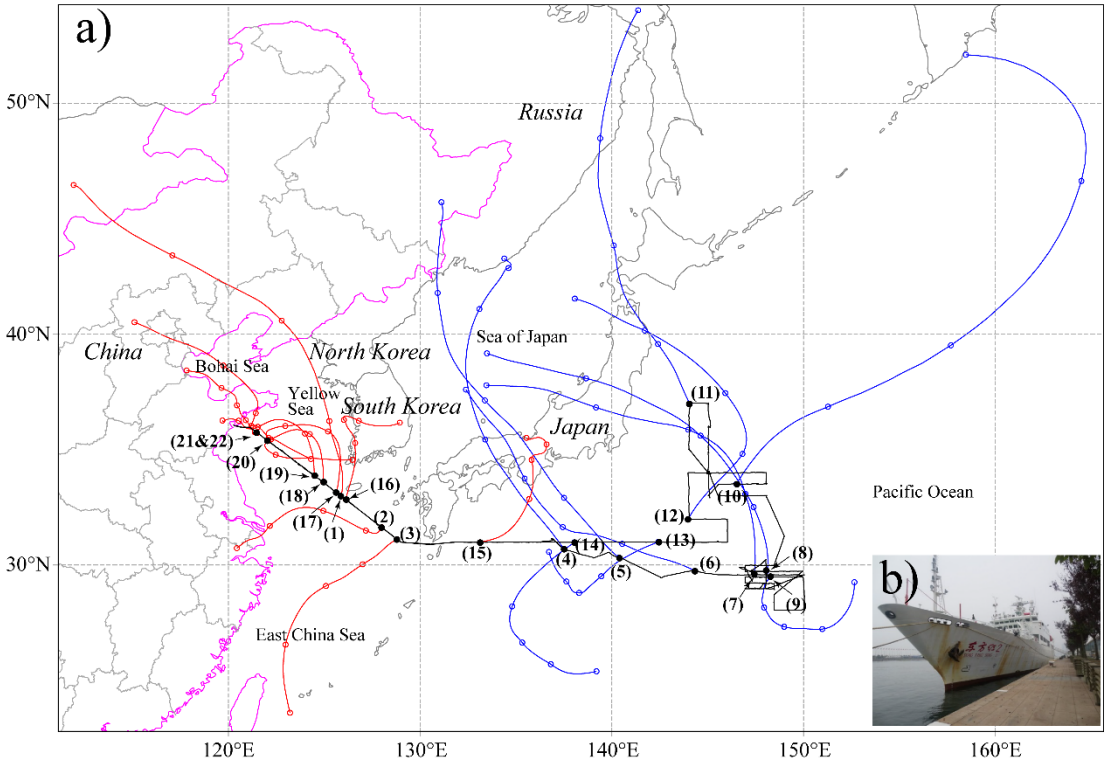

Figure 1. (a) Map of the cruise track (black line) and 48 h air mass backward trajectories (red and blue lines) arriving at 500 m above ground level at sampling locations. The interval between two circle symbols is 12 h. The number represents the sample ID in Table S1. (b) Photo of the R/V Dongfanghong 2.

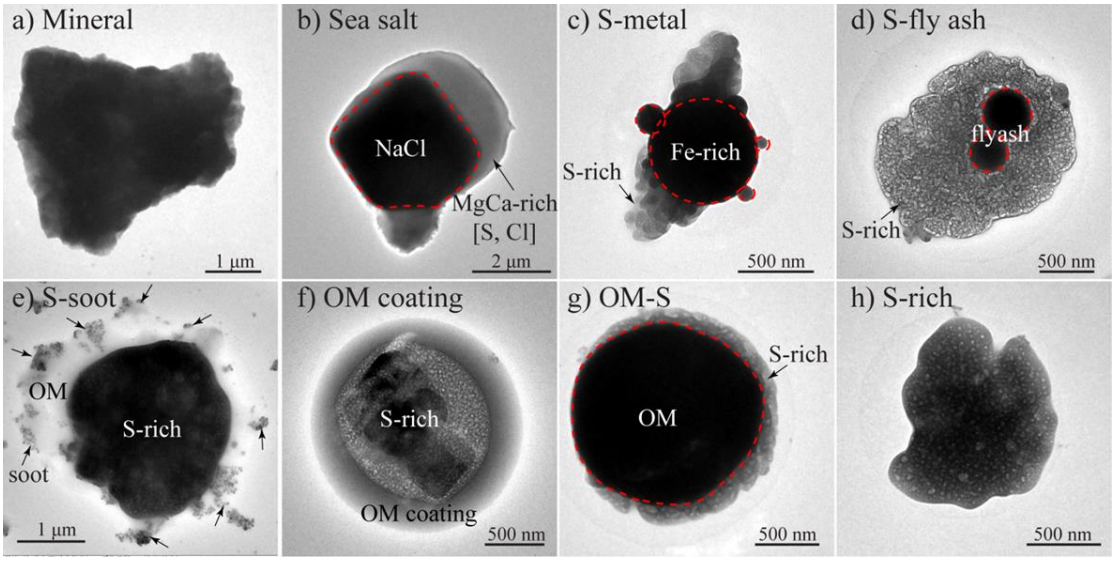

Figure 2. Transmission electron microscope (TEM) images of different types of aerosol particles: (a) mineral; (b) sea salt; (c) metal particles mixed with sulfate; (d) fly ash particles mixed with sulfate; (e) soot particles mixed with sulfate; (f) secondary organic matter (OM) coating on sulfate; (g) primary OM particle mixed with sulfate; (h) S-rich particle.

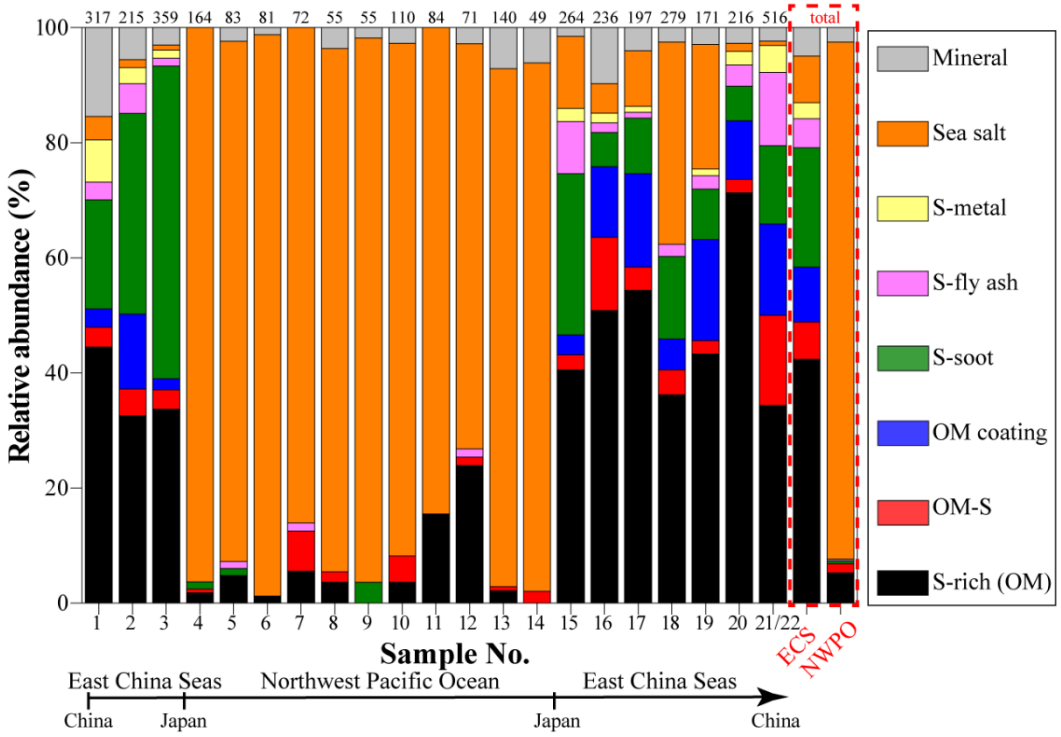

Figure 3. Relative abundances of eight types of aerosol particles in different samples. The number of analyzed aerosol particles is shown above the column.

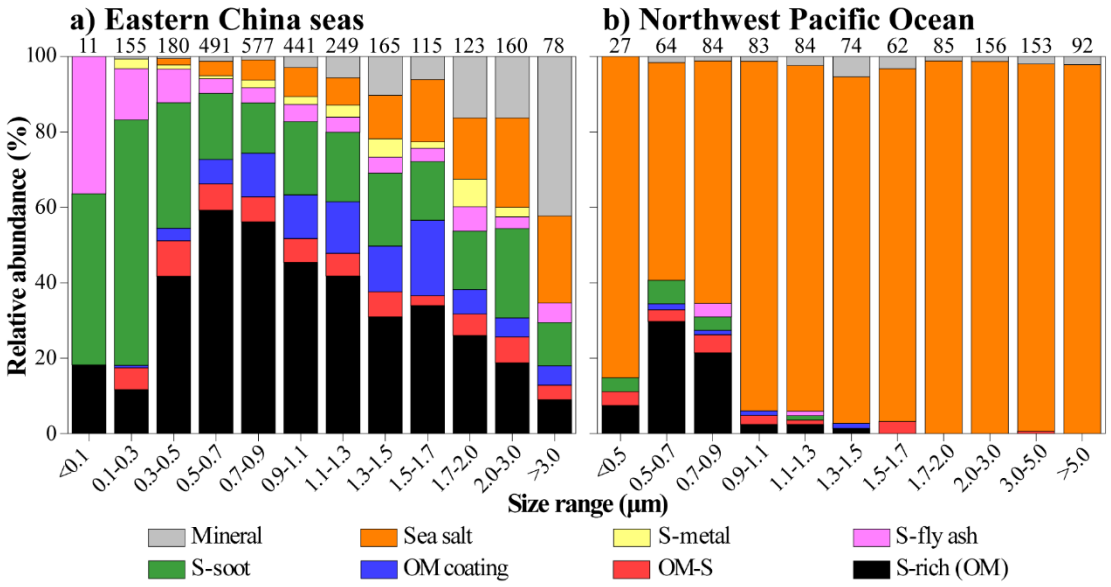

651

652 Figure 4. Relative abundances of individual particles in different size bins.

653

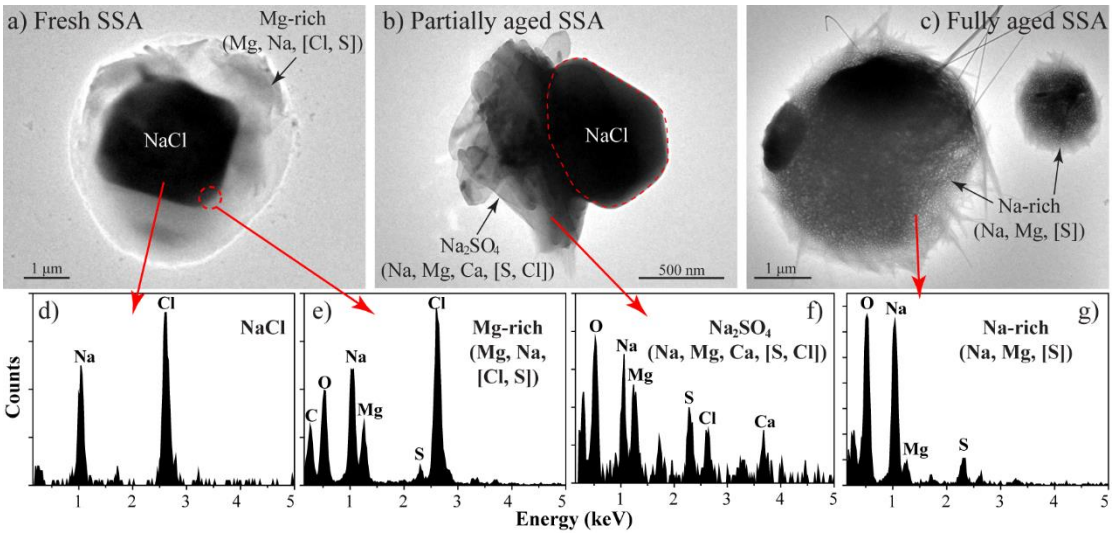

654

655 Figure 5. Morphology and EDS spectra of the typical fresh, partially aged, and fully

656 aged SSA. The main anionic elements are shown in the square brackets.

657

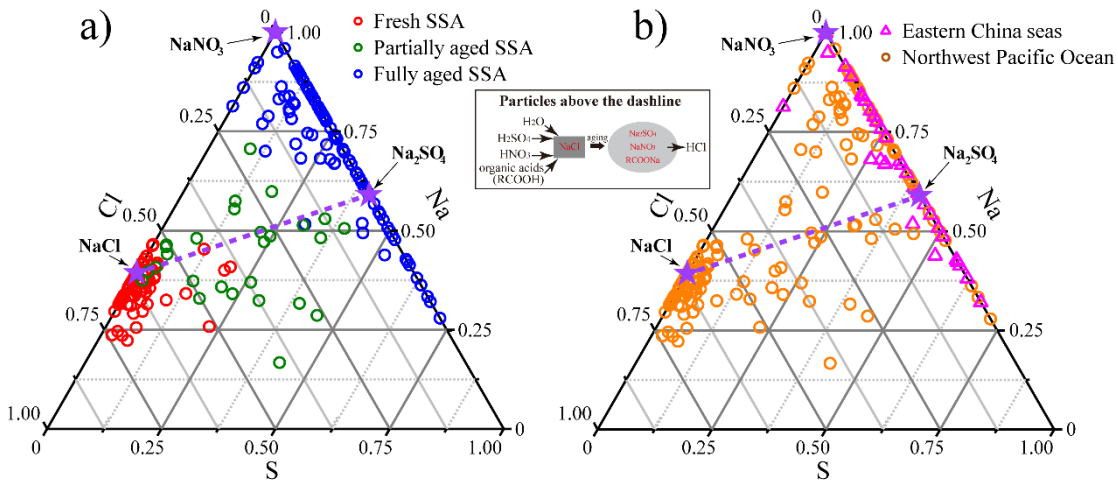

Figure 6. Triangular diagram of Na-Cl-S from EDS data (weight percentage) showing the elemental composition of SSA particles. The three stars represent pure NaCl, Na_2SO_4, and $NaNO_3$, respectively. The dash line indicates that Na:Cl:S is changed only by the postulated reaction of $2NaCl + H_2SO_4 \rightarrow Na_2SO_4 + 2HCl(g)$ (Zhang et al., 2003). Particles above the dash line are those which S cannot compensate Cl losses and there should be other processes causing Cl-depletion.

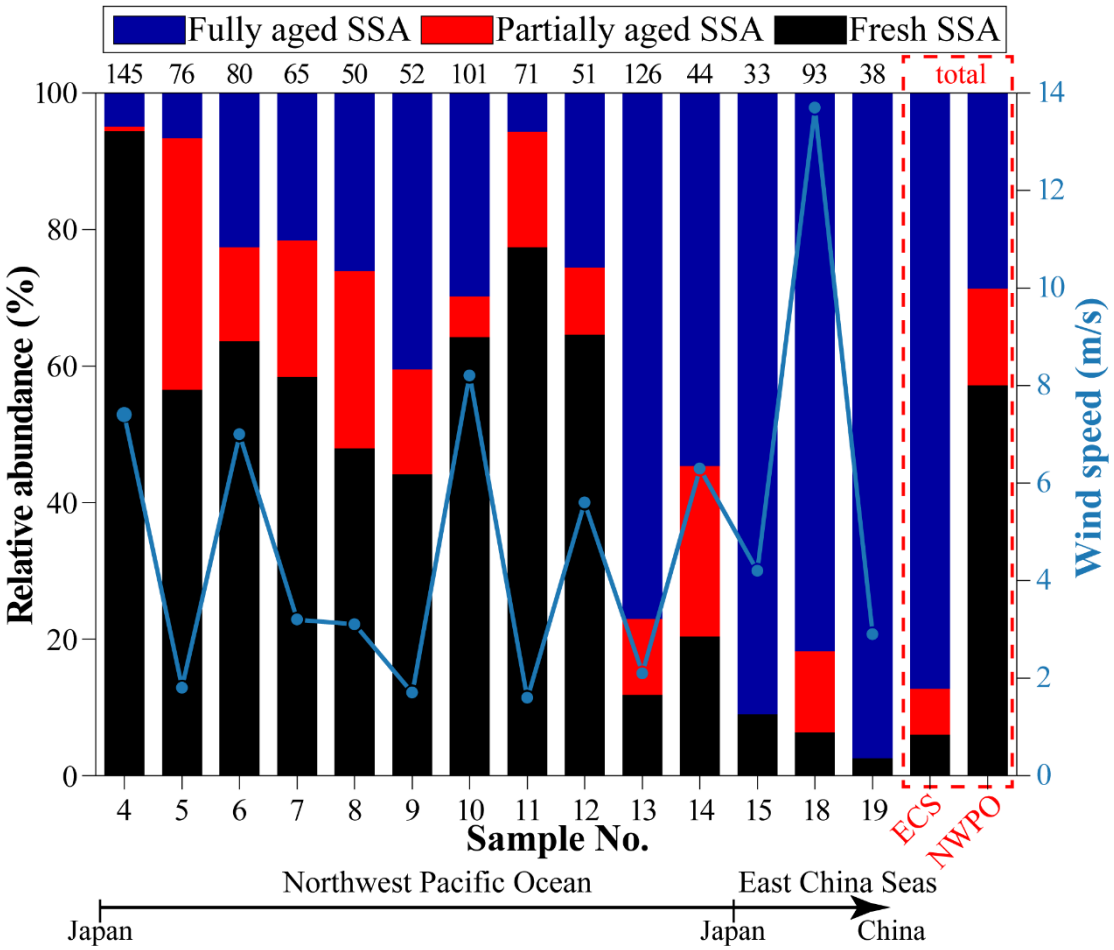

Figure 7. Relative abundances of the fresh, partially aged, and fully aged SSA particles in different samples. Samples with SSA particle less than 30 are excluded due to the small number. The line indicates the wind speed of the corresponding sample.

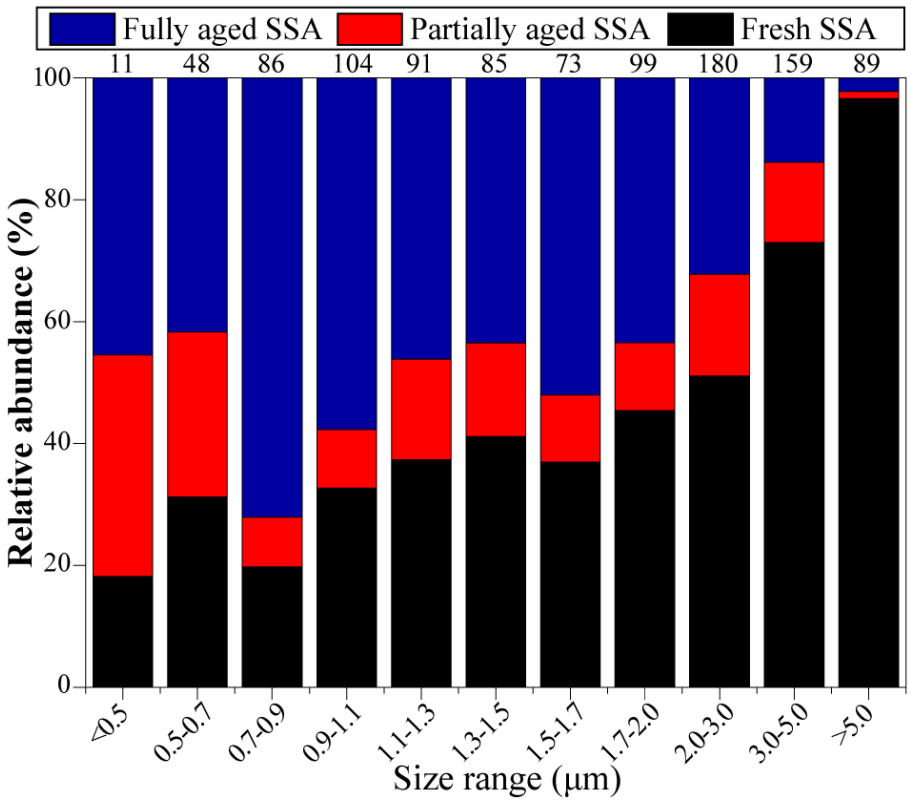

672

673 Figure 8. Relative abundances of three types of SSA particles in different size bins

674

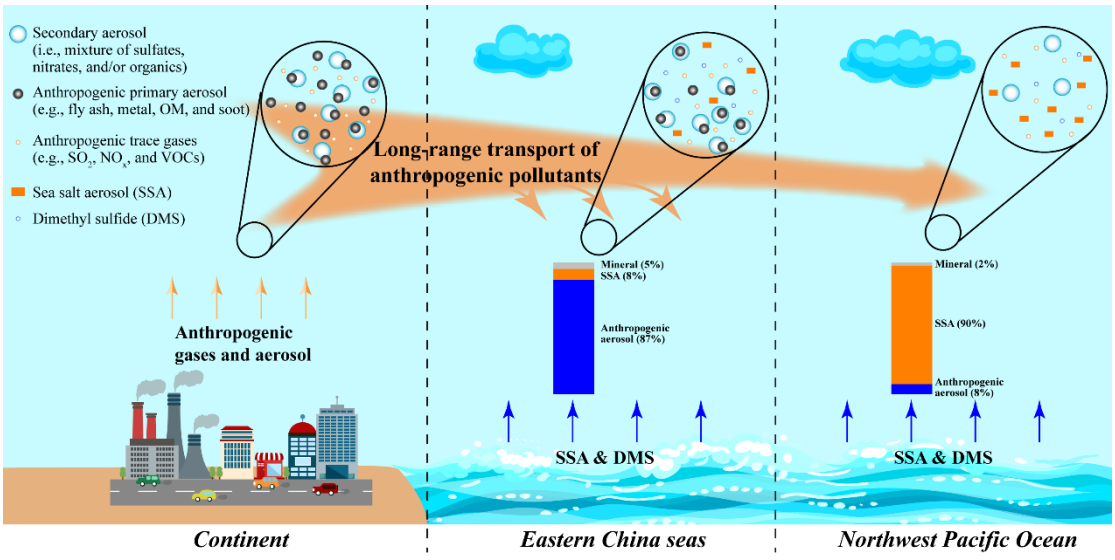

675

676 Figure 9. Schematic diagram showing the impact of long-range transported

677 anthropogenic air pollutants on marine aerosols

678